Studies of the Solid-State Conformation of Polysilaethylene: An Organic/Inorganic Hybrid Polymer with an Alternating C/Si Backbone

Mei-Wei Tsao,*,† Karl-Heinz Pfeifer, and John F. Rabolt†

IBM Almaden Research Center, San Jose, California 95120-6099

D. B. Holt and B. L. Farmer

Department of Materials Science and Engineering, University of Virginia, Charlottesville, Virginia 22903-2442

Leonard V. Interrante and Qionghua Shen

Department of Chemistry, Rensselaer Polytechnic Institute, Troy, New York 12180-3590

Received February 21, 1996; Revised Manuscript Received July 8, 1996[⊗]

ABSTRACT: Polysilaethylene ($[SiH_2CH_2]_n$) (PSE) and deuterated polysilaethylene ($[SiD_2CH_2]_n$) have been examined by both vibrational spectroscopy and X-ray diffraction methods above and below the crystallization/melting transition at −20 °C. The results confirm previous indications that PSE crystallizes in an all-trans conformation analogous to that found for its all-carbon analog, polyethylene. Raman spectroscopy reveals the appearance of a sharp band at 706 cm^{-1} attributable to the symmetric Si−C stretching vibration when PSE is cooled below 0 °C, while wide-angle X-ray diffraction shows the existence of a crystalline form with a monoclinic unit cell (a = 5.70 Å, b = 8.75 Å, c = 3.25 Å; γ = 97.5°) whose dimensions compare closely to the calculated repeat distance using the planar zigzag conformation of PSE. The calculation of the IR spectra by ab initio methods (Hartree−Fock level of theory) using the 3-21G* and 6-31G* basis sets agrees well with the experimental IR results. Through the use of the calculated IR spectra, symmetry analysis, and spectroscopic data on the deuterated sample, the assignments of the different PSE vibrational bands have been achieved.

Introduction

Among the linear polymers which contain silicon atoms in their backbones, the polycarbosilanes have been the least studied, despite their unique position in relation to the all-carbon (polyolefin) and all-silicon (polysilane) backbone polymers. The simplest example of the linear polycarbosilanes is poly(silylenemethylene) or polysilaethylene ($[SiH_2CH_2]_n$) (PSE), which can be viewed as a hybrid of the prototypical all-organic polymer, polyethylene $[CH_2CH_2]_n$, and the all-inorganic polysilane, $[SiH_2SiH_2]_n$.[1] In addition to the interest in PSE as an analog of PE and the parent member of an emerging family of poly(silylenemethylenes),[2−6] this polymer is also of interest as a precursor to silicon carbide,[7] an important ceramic material. The recent synthesis of PSE in a pure, high molecular weight form via the ring-opening polymerization of tetrachlorodisilacyclobutane[4] has now made it available for detailed study, and preliminary results[5] have provided ample justification for such a study, both as a SiC precursor and as a novel hybrid inorganic/organic polymer.

Preliminary studies of PSE by thermal analysis (DSC and TGA[4]), NMR, and ab initio Hartree−Fock calculations[5] have suggested (1) a relatively low (compared to PE) torsional barrier for the PSE chains, leading to an unusually low T_m (and probably T_g); (2) the presence of a crystalline phase below 0 °C, in which the chains appear to assume an all-trans conformation, by analogy to the ^{13}C NMR data of PE; and (3) thermal decomposition above ca. 200 °C to produce stoichiometrically pure SiC in a ceramic yield (86−90%) which approaches that expected for the loss of only H_2. This paper reports the results of a detailed study of the crystallization and the solid-state structure of PSE employing both vibrational spectroscopy and X-ray diffraction methods.

Experimental Section

A. Sample Preparation. The PSE used for this study was prepared by the H_2PtCl_6-catalyzed ring-opening polymerization of 1,1,3,3-tetrachloro-1,3-disilacyclobutane (TCDSCB), followed by reduction with $LiAlH_4$.[4,5] After workup by using aqueous HCl, the ether solution containing the PSE was evaporated under vacuum, leaving a viscous liquid. Pentane was used to redissolve the polymer. Then the pentane solution was filtered through a 0.45 μm filter, followed by removal of solvent under vacuum, giving a highly viscous, transparent, yellowish polymer in 78% yield from TCDSCB. Deuterated PSE, $[SiD_2CH_2]_n$, was made by the same process using $LiAlD_4$. Both polymers were fractionated before use by dissolving in benzene, followed by addition of methanol. The first fraction that precipitated (ca. 20% of the total amount of polymer) was employed for the measurements described herein.

For $[SiH_2CH_2]_n$: ^1H NMR (ppm) −0.15 (quintet, CH_2), 4.10 (quintet, SiH_2); $^{13}C\{H\}$ NMR (ppm) −9.2 ($SiCH_2Si$); $^{29}Si\{H\}$ NMR (ppm) −34.4 ($CSiH_2C$). M_n = 23 000; M_w = 71 000 (from GPC, refractive index detector, PS standards). For $[SiD_2CH_2]_n$: ^1H NMR (ppm) −0.15 (singlet, CH_2), 4.10 (vw quintet, SiHD); $^{13}C\{H\}$ NMR (ppm) −9.4 (CH_2); M_n = 27 400; M_w = 86 000 (from GPC).

The PSE obtained from the above synthesis procedure is a viscous liquid at room temperature and is soluble in most nonpolar organic solvents, such as benzene, toluene, pentane, and diethyl ether. It is relatively inert toward air since the "aqueous workup" that was carried out under air did not induce any measurable oxygen contamination.

B. Wide-Angle X-ray Diffraction. The diffraction patterns obtained at low temperature (5 °C) were recorded on flat photographic film in a Warhus camera. Low temperature was achieved by flowing methanol from a Neslab Endocal refrigerated circulating bath (ULT-80DD) through a copper block

† Current address: Materials Science Program, University of Delaware, Newark, DE 19716.

⊗ Abstract published in *Advance ACS Abstracts,* September 15, 1996.

S0024-9297(96)00267-7 CCC: $12.00

surrounding the sample holder. The camera was evacuated to reduce air scattering and ice buildup. Temperature control was obtained by cycling the control heater to the desired set point. A temperature stability of ±0.3 °C was attained. The sample was irradiated with nickel-filtered Cu Kα radiation. Exposure time was varied from 1 to 4.5 h.

C. IR Measurements. All the infrared measurements were made with an IBM/Bruker Model 98 evacuable FTIR at a resolution of 4 cm^{-1}. A spectral range from 400 to 4000 cm^{-1} was recorded. Samples were dissolved in benzene at a concentration of 1 mg/mL, and then the solution was spread onto zinc selenide substrates and allowed to dry. PSE/DPSE films prepared by the above method were used in all the FTIR measurements in this study. Reference spectra were taken from clean zinc selenide substrates. Each measurement consists of 600 scans which were then averaged to increase the S/N ratio. The low-temperature IR studies were carried out by using a liquid nitrogen-filled cold finger constructed in this laboratory.

D. Raman Studies. Raman spectra of all samples were recorded on an I.S.A. Jobin Yvon HG-2S scanning double monochromator using the 5145 Å output line of a Spectra-Physics 2020 water-cooled Ar^+ laser at an output level of 150 mW. An RCA 31034A-02 photomultiplier in conjunction with a Pacific Instrument Model 126 photometer−amplifier−discriminator module were used to detect the scattered photons. The spectral resolution was set at 2 cm^{-1} and the S/N ratio was enhanced by coaddition of 10−50 scans. The samples were positioned inside a 1.2 mm diameter capillary tube which could be held in a Harney-Miller cell for measurements at different temperatures.

E. Computational Chemistry. The quantum chemistry calculations were carried out on IBM RISC/6000 and SGI workstations using Mulliken,[8] a software package developed at the IBM Almaden Research Center. Due to the large amount of calculation required for both optimizing the molecular geometry and generating the vibrational spectrum (IR only) of a molecule, small molecules were used in these calculations rather than a true polymer chain. $H_3C-(SiH_2-CH_2)_3-SiH_2-CH_3$, $H_3C-(SiH_2-CH_2)_4-SiH_2-CH_3$, and $H_3C-(SiH_2-CH_2)_5-SiH_2-CH_3$ are here referred to as a "4 and half mer", "5 and half mer", and "6 and half mer", respectively. These were used as model systems for PSE. The geometry of the smallest molecule was first optimized at the Hartree−Fock level with the 3-21G* basis set,[9] making use of the symmetry of the molecule. Then the vibrational spectrum was calculated with the energy surface generated by the geometry optimization process. In a second run, the same procedures were repeated using the 6-31G* basis set.[10] If the two sets of spectra were close, the size of the model molecule was augmented by adding more monomeric units and spectra calculated by both the 3-21 G* and 6-31 G* basis sets were compared again.

Results and Discussion

I. Vibrational Assignments

A. PSE and DPSE. The CH stretching region (3100−2800 cm^{-1}) of both the IR and Raman spectra of PSE is considerably simplified due to the lack of CH_3 groups. Two medium to strong bands are observed in the low-temperature Raman spectrum, shown in Figure 1, at 2915 and 2875 cm^{-1} while the IR spectrum, as shown in Figure 3, contains two weak features at 2921 and 2881 cm^{-1} with a third broader, weaker feature at 2961 cm^{-1}. The latter feature, resulting from Fermi resonance interactions, is known to add complexity to this region.[11] Snyder has shown that Fermi resonance interaction is affected by the interchain coupling which causes lateral dispersion of the CH_2 bending modes.[11] The effect is to broaden the component bands and to make the C−H stretching region to some extent dependent on the chain packing.

As seen in Figures 1−3, deuteration of the $-SiH_2-$ groups has a dramatic effect on both the IR and Raman spectra of PSE, and the observed isotopic shift of bands can be utilized to make tentative band assignments. The most dramatic effect is found in the Raman spectra of PSE and DPSE, where the band at 2125 cm^{-1} in PSE is observed to shift to 1554 cm^{-1} in DPSE. This band can be confidently assigned to the symmetric $-SiH_2-$ stretching vibration. The strong band at 2120 cm^{-1}, which shifts to 1542 cm^{-1} upon deuteration, can be assigned to the asymmetric SiH_2 stretch. The same two

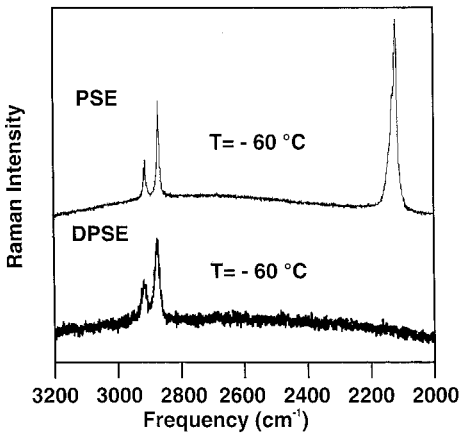

Figure 1. Solid-state Raman spectra of PSE and DPSE, 2000−3200 cm^{-1}.

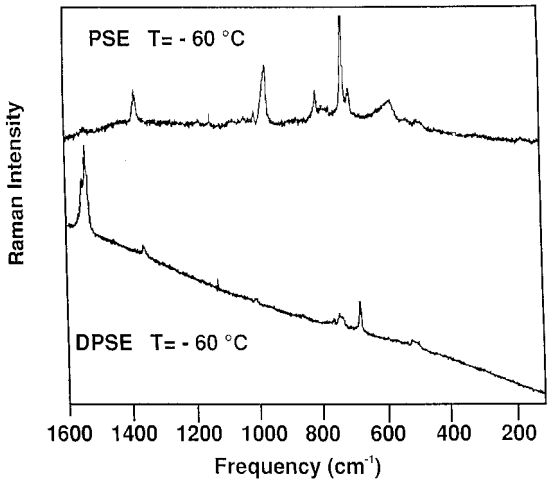

Figure 2. Solid-state Raman spectra of PSE and DPSE, 100−1600 cm^{-1}.

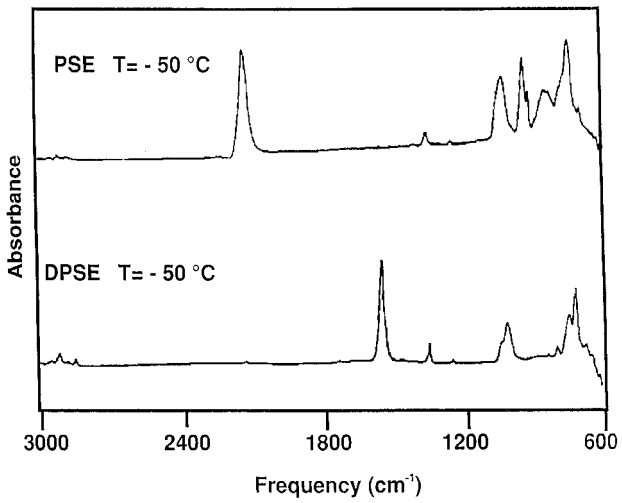

Figure 3. Solid-state IR spectra of PSE and DPSE, 600−3000 cm^{-1}.

bands are very intense in the IR spectrum shown in Figure 3 and although not completely resolved, both are observed to shift from about 2130 to 1554 cm^{-1} upon deuteration, confirming this assignment.

In the 1400−1100 cm^{-1} region, a number of weak bands are found, including that at 1356 cm^{-1}, which is observed at the same position in both the Raman and IR of PSE and DPSE. This clearly indicates that this vibration is not associated with the SiH_2 group and instead can be assigned to a CH_2 scissors vibration. Weak bands were also observed at 1406 and 1250 cm^{-1} in the IR spectra of both PSE and DPSE but their assignment is more speculative and will be discussed in the context of ab initio calculations described in a later section.

In the spectral region which extends from 1100 to 600 cm^{-1}, a number of intense bands are observed in both the IR and Raman spectra of PSE. The weak Raman band at 1030 cm^{-1} corresponds to the strong band at 1036 cm^{-1} in the IR spectrum and it remains unchanged upon deuteration. Hence this band can be assigned to the wagging mode of an isolated CH_2 group by comparison to poly(oxymethylene), $[CH_2O]_n$. On the other hand, the strong IR band at 946 cm^{-1} is found to shift to 688 cm^{-1} upon deuteration, and this behavior is consistent with this vibration being assigned to the SiH_2 scissors mode. In the low-temperature Raman spectrum shown in Figure 2, a very intense band is found at 706 cm^{-1} and its intensity is suggestive of the symmetric Si−C stretching mode observed in the planar zigzag form of poly(di-*n*-hexylsilane).[12] Upon deuteration, this band shifts to 669 cm^{-1}, mirroring similar behavior as that observed in the polysilanes and hence favoring this assignment. In a similar fashion, the strong band found at 756 cm^{-1} in the IR, with its corresponding weaker analogue at 749 cm^{-1} in the Raman, is observed at 730 cm^{-1} in DPSE and can be confidently assigned to the asymmetric Si−C stretch.

The remaining intense band in this region is found at 856 cm^{-1} in the IR, with no corresponding mode in the Raman and is observed to shift to 540 cm^{-1} in DPSE. It is assigned to a combination of SiH_2 twisting and wagging. These assignments (listed in Table 1) are consistent with known CH_2 and SiH_2 band assignments.[13] However, the assignments of many other PSE bands have never been attempted, and therefore a quantum chemistry approach was taken in this study to clarify these assignments and will now be discussed in the following section.

B. Quantum Chemistry Calculations. In order to refine the vibrational assignments in the IR and to test the effectiveness of quantum chemistry calculations in accurately predicting intensities, numerous calculations using various system sizes and basis sets at the Hartree−Fock level were undertaken. The largest system calculated in this study is the 6 and half mer using the 3-21G* basis set. However, after comparing calculation results based on different system sizes and basis sets with the experimental IR data, it was concluded that using larger basis sets is critical for getting frequency results close to the experimental data. Therefore, the results from the 5 and half mer system calculated with the 6-31G* basis set were used to compare with the experimental data. The result is shown in Figure 4, where the frequencies have all been scaled by 0.89 from the raw data of the calculation because SCF harmonic vibrational frequencies determined at this level of theory typically overestimate the

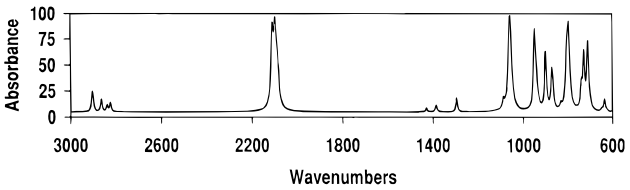

Figure 4. IR spectra obtained by ab initio calculation using "5 and half mer" system with the 6-31G* basis set.

Table 1. Vibrational Band Assignments for PSE in the Solid State

experimental		calculation	
Raman (cm^{-1})	IR (cm^{-1})	IR (cm^{-1})	assignment
	2961 vvw		
2915 m	2921 w	2865	asym CH_2 stretch
2875 vs	2881 vw	2825	sym CH_2 stretch
2125 vs	2130 vs	2108	sym SiH stretch
2120 vs	2126 sh	2057	asym SiH stretch
1528 vw			
	1406 vw	1430	CH_3 wag
1356 m	1353 m	1387	CH_2 scissors
	1250 vw	1296	$SiCH_3$ bend
1030 w	1036 s	1060	CH_2 wag
983 vw			
946 m	946 s	949	SiH_2 scissors
	925 s	901	SiH_2 wag
	856 m	868, 874	SiH_2 wag/twist
	840 m	798, 805	SiH_2 wag/twist
789 w			asym SiC stretch
749 vvw	756 vs	730, 741	asym SiC stretch nonplanar
706 vs			sym SiC stretch
686 w			
600 sh			
558 m			SiH_2 twist rock
472 vw			

observed fundamentals by an average of 12%.[14,15] The major difference between the calculated IR spectra and the experimental data is that the vibrational modes related to CH_3 terminal groups show up much stronger in the calculation of small-molecule systems than they would in the polymer system. This is due to the higher CH_3 end group concentration relative to CH_2 in small molecules than in the high molecular weight PSE. There is no notable difference in the calculated spectra for the three systems of different sizes, although upon close scrutiny, some bands do show a trend which gets closer to the experimental values as the system size increases. This observed size dependence of the oligomeric systems reflects the shape of the vibrational dispersion curve for the infinite chain.[16] Both the absence of dramatic size dependence and the agreement with the experimental IR spectra shown in Figure 3 indicate that this calculation scheme is quite accurate in describing the PSE chain.

Once the robustness of the calculations is established, the result shown in Figure 4 can be further used for the assignment of the PSE spectra. The method used for finding the vibrational modes for different bands is based upon one of the features of Mulliken's graphic user interface which allows dynamic viewing of each calculated mode. By studying the position of each atom as a function of time, i.e., the "animated" version of the calculated data, the atomic displacement associated with any calculated vibrational frequency can be identified. For example, the band at 946 cm^{-1} in both the IR and Raman spectra, assigned as SiH_2 bending, is shown to be due to a scissoring motion of the H−Si−H by this method, and the calculated frequency for this mode, 949 cm^{-1} (after scaling), is within 5 cm^{-1} of the experimental

Table 2. Symmetry Species for Possible PSE Conformations

conformation	symmetry group	symmetry species properties
planar	C_{2v}	$5A_1 + 2A_2 + 3B_1 + 4B_2$ IR, R R IR, R IR, R
TGTG′	C_{2h}	$10A_g + 7B_g + 7A_u + 8B_u$ R R IR IR
TTTGTTTG′	C_s	$34A' + 34A''$ IR, R IR, R

value. Table 1 lists the band assignments for the solid-state PSE based on both experimental data and the results from calculation. One can see that the CH_2 scissoring band at 1387 cm^{-1} is much weaker in the calculated spectrum than in the experimental data (at 1353 cm^{-1}), which is again due to the much lower CH_2/CH_3 concentration ratio in 5 and half mer than in PSE. The bands between 800 and 1000 cm^{-1} were found to be related to the SiH_2 twisting and wagging, consistent with the selective frequency shift observed in the DPSE spectrum in Figure 3.

Due to the lack of information on the polarizability derivatives, Mulliken is currently not able to calculate the Raman intensities with high accuracy. However, even though our spectral calculation method features only the intensities of the IR-active vibrational modes, the frequencies of all vibrational bands, i.e., both IR- and Raman-active bands, were calculated by the ab initio process. Therefore both the frequency and vibrational mode of a Raman-active mode can still be identified by the use of the dynamic viewing feature of Mulliken. The 706 cm^{-1} band in the low-temperature Raman spectra is thus identified as the symmetric stretching of Si−C in a planar zigzag conformation. The calculated frequency for this mode is 707 cm^{-1} and its intensity is finite, but too low to be seen on the same scale used for the IR-active bands shown in Figure 3. However, this result does indicate that the appearance of the sharp band at 706 cm^{-1} is due to the onset of the planar zigzag conformation of PSE in the solid state, in excellent agreement with our assignment.

C. Symmetry Analysis. From a symmetry point of view, PSE is very similar to poly(vinylidene fluoride) ($[CF_2CH_2]_n$, abbreviated as PVF2); therefore we utilized the same symmetry argument for PSE as previously described for PVF2 by Tadokoro et al.[17−19] Table 2 shows the numbers of Raman- and IR-active modes for different symmetry species corresponding to the three most likely chain conformations for PVF2 (and potentially for PSE). From Table 2, we can see that only the planar zigzag and TTTGTTTG′ conformations will give rise to vibrational modes which are both IR- and Raman-active. Since the experimentally observed spectra showed bands which are both Raman- and IR-active, such as the Si−H band at 2130 cm^{-1} in the IR, which also shows up in the Raman at 2125 cm^{-1}, we can thus eliminate the possibility of a TGTG′ chain conformation. On the other hand, again from Table 2, all bands from a TTTGTTTG′ conformation should be both Raman- and IR-active; i.e., all IR bands should be present in the Raman spectrum, although with different intensities, if the sample under investigation has a TTTGTTTG′ conformation. This is inconsistent with the observation that not all bands show up in both IR and Raman spectra. Therefore, the vibrational spectra can only support the conformation of a planar zigzag structure for PSE at low temperatures. The result from this qualitative analysis based on symmetry arguments, though simple, again agrees very well with the planar zigzag PSE solid-state conformation obtained through the identification of the low-temperature planar zigzag Raman band at 706 cm^{-1} and by the quantitative analysis based on ab initio calculations.

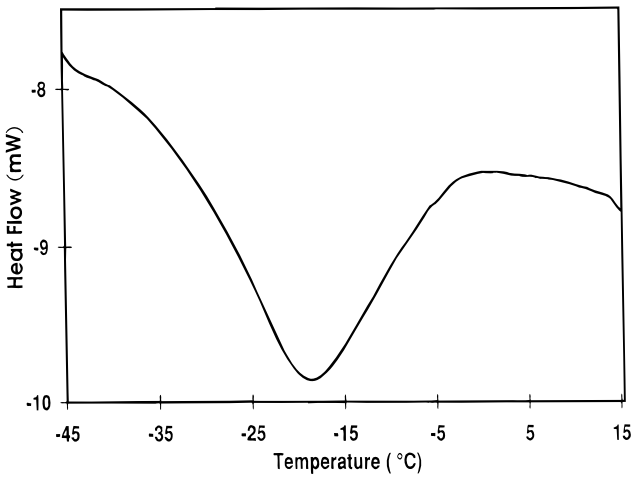

Figure 5. DSC thermogram of PSE obtained upon 10 °C/min heating.

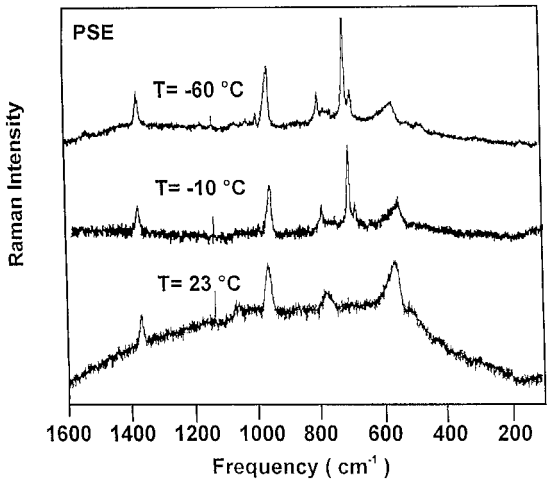

Figure 6. Raman spectra of PSE (100−1600 cm^{-1}) at different temperatures.

II. Nature of the Phase Transition

A. Thermal Analysis. DSC results shown in Figure 5 exhibit an endothermic transition at about −20 ± 5 °C with ΔH = 15.2 J/g. When this result is compared with the DSC results previously reported on PSE,[5] the peak in Figure 5 is as broad, but it shows up at a slightly different temperature. The broadness of the peaks in both cases is possibly due to a range of crystallite thickness and/or perfections. The difference in peak position, on the other hand, could be due to the different cooling/heating rate used. However, it is evident that there exists a phase transition in the vicinity of −20 °C, and as will be shown in the next section, it is the temperature at which a significant change in the Raman spectrum of PSE was observed.

B. Raman Spectroscopy. Figure 6 shows a series of three Raman spectra of PSE taken at different temperatures. The most notable change is that the sharp band at 706 cm^{-1} in the −10 and −60 °C spectra disappears at room temperature. DPSE shows the same behavior in that the 668 cm^{-1} band exists only in the

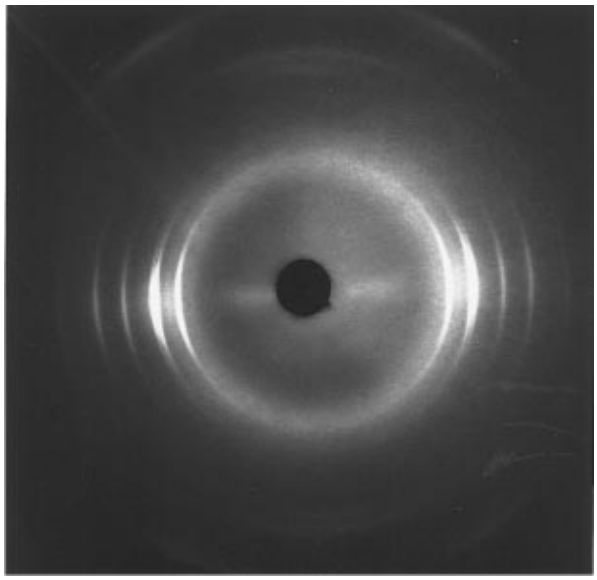

Figure 7. Low-temperature diffraction pattern of PSE.

Table 3. WAXD Equatorial Reflections

	d-spacing (Å)	
(*hk*0)	obsd	calcd
$1\bar{1}0$	5.00	5.05
110	4.37	4.47
020	4.27	4.34
$1\bar{2}0$	3.71	3.68
120	3.27	3.24
030	2.89	2.89

low-temperature spectra. In Figure 2, the 668 cm^{-1} band of DPSE seems to be lower in intensity than the PSE band at 706 cm^{-1}; this is due to the different scales used for the two spectra due to the presence of the very strong Si−D bands around 1540 cm^{-1} for DPSE. For both PSE and DPSE, this change of the Raman spectral feature is very similar to that found for the 689 cm^{-1} symmetric Si−C stretch in poly(di-*n*-alkylsilanes) reported by Rabolt et al.[12] In that case, the resonance-enhanced Si−C band at 689 cm^{-1} was used as the indicator for the planar zigzag conformation of poly(di-*n*-hexylsilane). Since in this study PSE does not show any UV−visible absorption between 190 and 800 nm both above and below the crystallization temperature, the 706 cm^{-1} Raman band is not resonance-enhanced like the 689 cm^{-1} band for poly(di-*n*-hexylsilane). Although the absolute population of the trans and gauche bonds cannot be determined unequivocally by the existence/absence of this Si−C stretching band, a similar spectroscopic approach may still be used in PSE as an indicator of the presence of the planar zigzag backbone conformation below the crystallization temperature.

C. Wide-Angle X-ray Diffraction. The wide-angle X-ray diffraction (WAXD) pattern obtained on an oriented fiber of PSE at 5 °C, shown in Figure7, showed six equatorial reflections and two reflections on the first layer line. From the measured layer line spacing, the *c* (chain axis) repeat distance was found to be 3.25 Å. As shown by the indexing in Table 3, the *hk*0 reflections are consistent with a monoclinic unit cell having dimensions $a = 5.70$ Å, $b = 8.75$ Å, $c = 3.25$ Å, and $\gamma = 97.5°$. Using values for the Si−C bond of 1.88 Å and 116° for the C−Si−C and Si−C−Si bond angles, the calculated repeat distance for a planar zigzag conformation of PSE is 3.19 Å. This agreement with the observed layer spacing confirms that the backbone conformation of PSE is indeed planar zigzag. The calculated density of the unit cell (0.913 g/cm^3) is typical of those measured for other silicon−carbon polymers such as poly(di-*n*-alkylsilanes).[12]

Conclusions

Vibrational spectroscopy and wide-angle X-ray diffraction methods, in conjunction with ab initio calculations, have been employed to characterize the solid-state conformation of polysilaethylene (PSE), a monosilicon analog of polyethylene and the parent member of a growing family of poly(silylenemethylenes). The existence of a phase transition at about −20 °C was also observed, below which the PSE backbone takes on a planar zigzag conformation. Thermal studies (DSC) reveal a single exothermic melting peak in the same temperature range. Many of the vibrational bands of PSE were identified by the combination of Raman and IR spectroscopy and assigned with the aid of symmetry analysis and ab initio quantum chemistry calculations. The sharp Raman band observed at 706 cm^{-1} upon cooling PSE below about −20 °C was found to be associated with the all-trans conformation of the polymer in its crystalline form. Wide-angle X-ray diffraction provided further verification for the all-trans, planar zigzag conformation. The combination of vibrational spectroscopy and X-ray diffraction constitutes a powerful method to characterize the structure of crystalline polymers and will be applied to other members of the poly(silylenemethylenes) family in the near future.

Acknowledgment. L.V.I. and Q.S. gratefully acknowledge the financial support of the National Science Foundation through Grant No. CHE-9520930. M.-W.T. and J.F.R. acknowledge the support and encouragement of Dr. H. Guard of the Office of Naval Research through Contract No. N00014-93-C-0105.

References and Notes

(1) (a) Damewood, J. R., Jr.; West, R. *Macromolecules* **1985**, *18*, 159. (b) Welsh, W. J.; DeBolt, L.; Mark, J. E. *Macromolecules* **1986**, *19*, 2978. (c) John, P.; Odeh, I. M.; Wood, J. *J. Chem. Soc., Chem. Commun.* **1983**, 1496.

(2) Bacque, E.; Pillot, J.-P.; Birot, M.; Dunogues, J. *Macromolecules* **1988**, *21*, 30, 34.

(3) Wu, H.-J.; Interrante, L. V. *Chem. Mater.* **1989**, *1*, 564.

(4) Wu, H.-J.; Interrante, L. V. *Macromolecules* **1992**, *25*, 1840.

(5) Interrante, L. V.; Wu, H.-J.; Apple, T.; Shen, Q.; Ziemann, B.; Narsavage, D. M.; Smith, K. *J. Am. Chem. Soc.* **1994**, *116*, 12085.

(6) Rushkin, I. L.; Interrante, L. V. *Macromolecules* **1995**, *28*, 5160.

(7) (a) Laine, R. M.; Babonneau, F. *Chem. Mater.* **1993**, *5*, 260. (b) Interrante, L. V.; Whitmarsh, C. W.; Sherwood, W.; Wu, H.-J.; Lewis, R.; Maciel, G. *Mater. Res. Soc. Symp. Proc.* **1994**, *346*, 593. (c) Interrante, L. V.; Whitmarsh, C. W.; Sherwood, W.; Wu, H.-J.; Lewis, R.; Maciel, G. *Application of Organometallic Chemistry in the Preparation and Processing of Advanced Materials*; Harrod, J. F., Laine, R. M., Eds.; NATO ASI Series 297; Kluwer Academic Publishers; Dordrecht, 1995; p 173.

(8) Mulliken: a computational quantum chemistry program developed at International Business Machines Corp. by J. E. Rice, H. Horn, B. H. Lengsfield, A. D. McLean, J. T. Carter, E. S. Replogle, L. A. Barnes, S. A. Maluendes, G. C. Lie, M. Gutowski, W. E. Rudge, S. P. A. Sauer, R. Lindh, K. Andersson, T. S. Chevalier, P.-O. Widmark, D. Bouzida, G. Pacansky, S. Singh, C. J. Gillan, P. Carnevali, W. C. Swope, and B. Liu.

(9) (a) Binkley, J. S.; Pople, J. A.; Hehre, W. J. *J. Am. Chem. Soc.* **1980**, *102*, 939. (b) Gordon, M. S.; Binkley, J. S.; Pople, J. A.; Pietro, W. J.; Hehre, W. J. *J. Am. Chem. Soc.* **1982**, *104*, 2797. (c) Pietro, W. J.; Francl, M. M.; Hehre, W. J.; Defrees, D. J.; Pople, J. A.; Binkley, J. S. *J. Am. Chem. Soc.* **1982**, *104*, 5039.

(10) Hariharan, P. C.; Pople, J. A. *Theor. Chim. Acta* **1973**, *28*, 213.

(11) Snyder, R. G.; Strauss, H. L.; Elliger, C. A. *J. Phys. Chem.* **1982**, *86*, 5145.

(12) KariKari, E. K.; Greso, A. J.; Farmer, B. L.; Miller, R. D.; Rabolt, J. F. *Macromolecules* **1993**, *26*, 3937.

(13) Lin-Vien, D.; Colthup, N. B.; Fateley, W. G.; Grasselli, J. G. *The Handbook of Infrared and Raman Characteristic Frequencies of Organic Molecules;* Academic Press: San Diego, 1991.

(14) Hehre, W. H.; Radom, L.; Schleyer, P. v. R.; Pople, J. A. *Ab Initio Molecular Orbital Theory;* Wiley: New York, 1986.

(15) Pople, J. A.; Head-Gordon, M.; Fox, D. J.; Raghavachari, K.; Curtiss, L. A. *J. Chem. Phys.* **1989**, *90*, 5622.

(16) Rabolt, J. F.; Fanconi, B. *Macromolecules* **1978**, *11*, 740.

(17) Hasegawa, R.; Kobayashi, M.; Tadokoro, H. *Polym. J.* **1972**, *3*, 591.

(18) Hasegawa, R.; Takahashi, Y.; Chatani, Y.; Tadokoro, H. *Polym. J.* **1972**, *3*, 600.

(19) Kobayashi, M.; Tashiro, K.; Tadokoro, H. *Macromolecules* **1975**, *8*, 158.

MA960267B